8. On the transitions from periodic to chaotic orbits in continual systems

Jan Awrejcewicz, V.A. Krysko, I.V. Papkova, A.V. Krysko, Jerzy Mrozowski

8.1. Introduction

One of the challenging directions of the continual system chaotic dynamics investigations is that of plates and shells dissipative dynamics, and in particular detection of the scenarios leading to chaos in those systems plays a crucial role both in theory and applications. Almost in all studied so far cases, the infinite dimensional objects (plates and shells) are modelled as one- and/or two-degrees-of-freedom systems. In contrary, here we deal with the infinitely dimensional problem, which is solved by qualitatively different numerical approaches including the Bubnov-Galerkin method (BGM) and the Ritz method (RM) in higher approximations, as well as the Finite Difference Method (FDM) with various space coordinates partition. This approach will validate both suitability of the numerical algorithms as well allows to trace scenarios leading to chaos in continual mechanical systems, cf. Awrejcewicz, Krysko V.A. and Valakis (2004), Awrejcewicz, Krysko V.A. and Krysko A.V. (2007), Awrejcewicz and Krysko V.A. (2008), Volmir (1967), Kantor (1971).

8.2. Mathematical models of continual mechanical systems

We study a shallow shell occupied a subspace of the 3D space in R^3 with the curvature system of coordinates x, y, z introduced in the following way. In the shell body (for z=0) the middle shell surface is fixed. Axes Ox and Oy are

directed along main curvatures of that surface, whereas axis Oz goes into the curvature centre. In the so far described coordinates our shell as the 3D object Ω is defined as follows (see Smale (1962))

$$\Omega=\{x,y,z/(x,y,z)\in[0,\alpha]\times[0,\beta]\times[-h/2,h/2]\}.$$

We apply the Kirchhoff-Love hypothesis regarding straight normal and the governing equations have the following form

$$\begin{aligned}&\left[\frac{1}{\lambda^2}\frac{\partial^2 w}{\partial x^2}\frac{\partial^2(\cdot)}{\partial x^2}+\lambda^2\frac{\partial^2 w}{\partial y^2}\frac{\partial^2(\cdot)}{\partial y^2}+2(1-\mu)\frac{\partial^2 w}{\partial xy}\frac{\partial^2(\cdot)}{\partial xy}+\mu\left(\frac{\partial^2 w}{\partial x^2}\frac{\partial^2(\cdot)}{\partial y^2}+\frac{\partial^2 w}{\partial y^2}\frac{\partial^2(\cdot)}{\partial x^2}\right)\right]-\\&-\nabla_k^2F+p_x(t)\frac{\partial^2 w}{\partial y^2}+p_y(t)\frac{\partial^2 w}{\partial x^2}-L(w,F)+Mq(t)-\left(\frac{\partial^2 w}{\partial t^2}+\varepsilon\frac{\partial w}{\partial t}\right)=0,\\&\left[\left(\lambda^2\frac{\partial^2 F}{\partial y^2}-\mu\frac{\partial^2 F}{\partial x^2}\right)\frac{\partial^2(\cdot)}{\partial y^2}+\left(\frac{1}{\lambda^2}\frac{\partial^2 F}{\partial x^2}-\mu\frac{\partial^2 F}{\partial y^2}\right)\frac{\partial^2(\cdot)}{\partial x^2}+2(1+\mu)\frac{\partial^2 F}{\partial xy}\frac{\partial^2(\cdot)}{\partial xy}\right]+\\&+\nabla_k^2w+\tfrac{1}{2}L(w,F)=0,\end{aligned}\qquad(8.1)$$

where

$$L(w,F)=\frac{\partial^2 w}{\partial x^2}\frac{\partial^2 F}{\partial y^2}+\frac{\partial^2 F}{\partial x^2}\frac{\partial^2 w}{\partial y^2}-2\frac{\partial^2 w}{\partial xy}\frac{\partial^2 F}{\partial xy},\qquad \nabla_k^2=k_y\frac{\partial^2}{\partial x^2}+k_x\frac{\partial^2}{\partial y^2}.$$

We have introduced the following non-dimensional quantities: $w=h\overline{w}$, $F=Eh^2\overline{F}$, $t=t_0\bar{t}$, $\varepsilon=\overline{\varepsilon}/\tau$. For the case of the rectangular spherical panel and the cylindrical panel we have: $x=a\overline{x}$, $y=a\overline{y}$; $k_x=\overline{k}_xh/b^2$, $k_y=\overline{k}_yh/a^2$, $q=\overline{q}Eh^4/(a^2b^2)$, $p_x=\overline{p}_xEh^3/b^2$, $p_y=\overline{p}_yEh^3/a^2$, $\tau=abh^{-1}\sqrt{\rho(Eg)^{-1}}$, M=1, $\lambda=a/b$, where a, b are the shell dimensions regarding x and y, respectively; for the case of the closed cylindrical shell: $x=L\overline{x}$, $y=R\overline{y}$, $k_y=\overline{k}_yh/R^2$ (k_x=0), $q=\overline{q}Eh^4/(L^2R^2)$, $p_x=\overline{p}_xEh^3/R^2$, $\tau=LRh^{-1}\sqrt{\rho(Eg)^{-1}}$, $M=k_x^{\,2}$, $\lambda=L/R$, where L and $R=R_y$ are length and radius of the shell; t denotes time; ε is the damping coefficient, μ=0.3; $p_x(t)$, $p_y(t)$ are longitudinal loads; $q(x,y,t)$ is the transversal load. Farther, bars over non-dimensional quantities are omitted. One of the following boundary conditions is attached to equations (8.1).

1. Free clamping of shell edges:

$$w=0;\quad \frac{\partial w}{\partial x}=0;\quad F=0;\quad \frac{\partial F}{\partial x}=0\qquad \text{for}\qquad x=0,1,\qquad(8.2)$$
$$w=g(x,y,t);\quad \frac{\partial w}{\partial y}=p(x,y,t);\quad F=u(x,y,t);\quad \frac{\partial F}{\partial y}=v(x,y,t)\qquad \text{for}\qquad y=0,\xi.$$

2. Free support on shell edges:

$$w=0;\quad \frac{\partial w}{\partial x}=0;\quad F=0;\quad \frac{\partial^2 F}{\partial x^2}=0\qquad \text{for}\qquad x=0,1,\qquad(8.3)$$
$$w=g(x,y,t);\quad \frac{\partial w}{\partial y}=p(x,y,t);\quad F=u(x,y,t);\quad \frac{\partial F}{\partial y}=v(x,y,t)\qquad \text{for}\qquad y=0,\xi.$$

3. Free clamping of shell edges with ribs:

$$w=0;\quad \frac{\partial^2 w}{\partial x^2}=0;\quad F=0;\quad \frac{\partial F}{\partial x}=0\qquad \text{for}\qquad x=0,1,\qquad(8.4)$$
$$w=g(x,y,t);\quad \frac{\partial w}{\partial y}=p(x,y,t);\quad F=u(x,y,t);\quad \frac{\partial F}{\partial y}=v(x,y,t)\qquad \text{for}\qquad y=0,\xi.$$

4. Free clamping of shell edges with flexible ribs:

$$w=0;\quad \frac{\partial^2 w}{\partial x^2}=0;\quad F=0;\quad \frac{\partial^2 F}{\partial x^2}=0\qquad \text{for}\qquad x=0,1,\qquad(8.5)$$
$$w=g(x,y,t);\quad \frac{\partial^2 w}{\partial y^2}=r(x,y,t);\quad F=u(x,y,t);\quad \frac{\partial^2 F}{\partial y^2}=z(x,y,t)\qquad \text{for}\qquad y=0,\xi.$$

Here and further we take $\xi=2\pi$ for the closed cylindrical shell, and ξ=1 for the rectangular panel. Observe that non-homogeneous boundary conditions (for y=0,ξ) indicate the initial imperfections and stresses occurred in the shell. Finally, the following initial conditions are attached to equations (8.1):

$$w|_{t=0}=w_0,\qquad \dot{w}|_{t=0}=0.\qquad(8.6)$$

A solution governing dynamics of the closed cylindrical shell has been found using the Bubnov-Galerkin approach in higher approximations, whereas for the case of rectangular spherical shell a solution is sought through two methods independently, i.e. using BGM and FDM.

In order to find solutions to equation (8.1) using BGM the functions w and F are approximated by analytical expression consisting of a finite number of arbitrary parameters, being the solution composed as a product of the functions depending on time and space of the form

$$w=\sum_{i=0}^{N_1}\sum_{j=0}^{N_2}A_{ij}(t)\varphi_{ij}(x,y),\qquad F=\sum_{i=0}^{N_1}\sum_{j=0}^{N_2}B_{ij}(t)\psi_{ij}(x,y).\qquad(8.7)$$

The coefficients $A_{ij}(t)$ and $B_{ij}(t)$ are being sought time functions. Application of the BGM yields:

$$\sum_{rs}\Bigg[\sum_{ij}A_{ij}\sum_{kl}H_{ijklrs}+\sum_{ij}B_{ij}C_{1,ijrs}+\sum_{ij}A_{ij}W_{ijrs}+MqQ_{rs}+$$
$$+\sum_{ij}A_{ij}\sum_{kl}B_{kl}D_{1,ijklrs}+\sum_{ij}\left[\frac{d^2A_{ij}}{dt^2}+\varepsilon\frac{dA_{ij}}{dt}\right]G_{ijrs}\Bigg]=0, \tag{8.8}$$
$$\sum_{rs}\Bigg[\sum_{ij}A_{ij}C_{2,ijrs}+\sum_{ij}B_{ij}\sum_{kl}P_{ijklrs}+\sum_{ij}A_{ij}\sum_{kl}A_{rs}D_{2,ijklrs}\Bigg]=0.$$

In the above $\sum_{rs}[*]$ means that instead of each one of equations of (8.8) we take rs such equations, and the associated integrals of the BGM follow:

$$H_{ijklrs}=\int_0^1\int_0^\xi\frac{1}{12(1-\mu^2)}\left[\frac{1}{\lambda^2}\frac{\partial^2\varphi_{ij}}{\partial x^2}\frac{\partial^2\varphi_{kl}}{\partial x^2}+\lambda^2\frac{\partial^2\varphi_{ij}}{\partial y^2}\frac{\partial^2\varphi_{kl}}{\partial y^2}+2\frac{\partial^2\varphi_{ij}}{\partial x\partial y}\frac{\partial^2\varphi_{kl}}{\partial x\partial x}\right]\varphi_{rs}dxdy,$$
$$C_{1,ijrs}=\int_0^1\int_0^\xi\left[-k_y\frac{\partial^2\psi_{ij}}{\partial x^2}-k_x\frac{\partial^2\psi_{ij}}{\partial y^2}\right]\varphi_{rs}dxdy,\quad C_{2,ijrs}=\int_0^1\int_0^\xi\left[k_y\frac{\partial^2\varphi_{ij}}{\partial x^2}+k_x\frac{\partial^2\varphi_{ij}}{\partial y^2}\right]\psi_{rs}dxdy,$$
$$D_{1,ijklrs}=\int_0^1\int_0^\xi\left[-L(\varphi_{ij},\psi_{kl})\right]\varphi_{rs}dxdy,\quad D_{2,ijklrs}=\int_0^1\int_0^\xi\frac{1}{2}L(\varphi_{ij},\varphi_{kl})\psi_{rs}dxdy,$$
$$P_{ijklrs}=\int_0^1\int_0^\xi\left[\frac{1}{\lambda^2}\frac{\partial^2\psi_{ij}}{\partial x^2}\frac{\partial^2\psi_{kl}}{\partial x^2}+\lambda^2\frac{\partial^2\psi_{ij}}{\partial y^2}\frac{\partial^2\psi_{kl}}{\partial y^2}+2\frac{\partial^2\psi_{ij}}{\partial x\partial y}\frac{\partial^2\psi_{kl}}{\partial x\partial x}\right]\psi_{rs}dxdy,$$
$$G_{ijrs}=\int_0^1\int_0^\xi\left[-\varphi_{ij}\varphi_{rs}\right]dxdy,\quad Q_{rs}=\int_{x_1}^{x_2}\int_{y_1}^{y_2}Mq(x,y,t)\varphi_{rs}dxdy, \tag{8.9}$$
$$W_{ijrs}=\int_0^1\int_0^\xi\left[p_y(x,t)\frac{\partial^2\varphi_{ij}}{\partial x^2}+p_x(y,t)\frac{\partial^2\varphi_{ij}}{\partial y^2}\right]\varphi_{rs}dxdy.$$

Integrals (8.9) (possibly in spite of Q_{rs}, if the transversal load will be applied to a part of the shell) are computed regarding the whole middle shell surface. After application of the BGM procedure the following matrix system of ODEs is obtained regarding $A_{ij}(t)$ and $B_{ij}(t)$:

$$\mathbf{G}(\ddot{\mathbf{A}}+\varepsilon\dot{\mathbf{A}})+\mathbf{HA}+\mathbf{WA}+\mathbf{C}_1\mathbf{B}+\mathbf{D}_1\mathbf{AB}=\mathbf{Q}q(t),$$
$$\mathbf{C}_2\mathbf{A}+\mathbf{PB}+\mathbf{D}_2\mathbf{AA}=0, \tag{8.10}$$

where $\mathbf{H}=\|H_{ijrs}\|$, $\mathbf{G}=\|G_{ijrs}\|$, $\mathbf{C}_1=\|C_{1ijrs}\|$, $\mathbf{C}_2=\|C_{2ijrs}\|$, $\mathbf{D}_1=\|D_{1ijklrs}\|$, $\mathbf{D}_2=$ $=\|D_{2ijklrs}\|$, $\mathbf{W}=\|W_{ijrs}\|$, $\mathbf{P}=\|P_{ijrs}\|$ – squared matrices of dimensions $2\cdot N_1\cdot N_2\times$ $\times 2\cdot N_1\cdot N_2$, $\mathbf{A}=\|A_{ij}\|$, $\mathbf{B}=\|B_{ij}\|$, $\mathbf{Q}=\|Q_{ij}\|$ – matrices of $2\cdot N_1\cdot N_2\times 1$.

Further, second equation of (8.10) is solved with respect to $\mathbf{B}$ via the inverse of a matrix on each computational step:

$$\mathbf{B}=\left[-\mathbf{P}^{-1}\mathbf{D}_2\mathbf{A}-\mathbf{P}^{-1}\mathbf{C}_2\right]\mathbf{A}. \tag{8.11}$$

Multiplying by $\mathbf{G}^{-1}$ the first equation of (8.10) and denoting $\dot{\mathbf{A}}=\mathbf{R}$, the following Cauchy problem is formulated:

$$\dot{\mathbf{R}}=-\bar{\varepsilon}\mathbf{R}-\left[\mathbf{G}^{-1}\mathbf{C}_1+\mathbf{G}^{-1}\mathbf{D}_1\mathbf{A}\right]\cdot\mathbf{B}-\mathbf{G}^{-1}\mathbf{HA}-\mathbf{G}^{-1}\mathbf{WA}+\mathbf{G}^{-1}\mathbf{Q}q(\bar{t}),$$
$$\dot{\mathbf{A}}=\mathbf{R}. \tag{8.12}$$

Note that inversed matrices $\mathbf{G}^{-1}$ and $\mathbf{P}^{-1}$ exist if the coordinate functions are linearly independent.

One of the boundary conditions (8.2)–(8.5) and the initial conditions (8.6) are attached to equations (8.12). The obtained first order ODEs are solved using the 4-th order Runge-Kutta method, whereas the computational step is chosen applying the Runge's rule.

8.3. Spherical and conical shallow shells

We study a shallow shell, which can be treated as the plate with initial imperfections occupying a closed part of R^3 with the introduced curvilinear system of coordinates α, β,γ, cf. Li and Yorke (1975). We assume that the Lamé parameters A, B and the radii R_1', R_{12}, R_2' of the middle shell surface as well as their first derivatives are continuous functions of α,β. In the given system of coordinates the shell treated as a 3D object Ω is defined by:

$$\Omega=\left\{\alpha,\beta,\gamma\ /\ (\alpha,\beta,\gamma)\in[0,a]\times[0,b]\times\left[-h/2,h/2\right]\right\}.$$

The corresponding variation equation is cast to the form

$$\delta\iint_S\left\{\frac{D}{2}\left[(\Delta w)^2-(1-\nu)L_2(w,w)\right]-\left[\Delta_k\varphi+L_2\left(\frac{1}{2}w+w_0,\varphi\right)\right]w-\right.$$
$$\left.-\frac{1}{2Eh}\left[(\Delta\varphi)^2-(1+\nu)L_2(\varphi,\varphi)\right]\right\}ds-\iint_S\left[q-\frac{h\gamma}{g}(\ddot{w}+\dot{w})\right]\delta w ds=0, \tag{8.13}$$

where $\Delta=\frac{1}{AB}\left(\frac{\partial}{\partial\alpha}\frac{B}{A}\frac{\partial}{\partial\alpha}+\frac{\partial}{\partial\beta}\frac{A}{B}\frac{\partial}{\partial\beta}\right)$, $\Delta_k=\frac{1}{AB}\left(\frac{\partial}{\partial\alpha}\frac{1}{R_1'}\frac{B}{A}\frac{\partial}{\partial\alpha}+\frac{\partial}{\partial\alpha}\frac{1}{R_{12}}\frac{\partial}{\partial\beta}+\right.$
$\left.+\frac{\partial}{\partial\beta}\frac{1}{R_{12}}\frac{\partial}{\partial\alpha}+\frac{\partial}{\partial\beta}\frac{1}{R_1'}\frac{A}{B}\frac{\partial}{\partial\beta}\right)$, $L(w,\varphi)=\frac{\partial^2 w}{\partial\alpha^2}\cdot\frac{\partial^2\varphi}{\partial\alpha^2}+2\frac{\partial^2 w}{\partial\alpha\partial\beta}\cdot\frac{\partial\varphi^2}{\partial\alpha\partial\beta}+\frac{\partial^2 w}{\partial\beta^2}\cdot\frac{\partial^2\varphi}{\partial\beta^2}$,
$D=\frac{Eh^3}{12(1-\nu^2)}$ – cylindrical stiffness; φ – stress function. The following non-dimensional parameters are introduced: $t=\bar{t}\tau$, $\varepsilon=\bar{\varepsilon}/\tau$, where $\tau=a(h_0)^{-1}\sqrt{a^2\gamma(Eg)^{-1}}$, $q_0(t)=q(t)a^4(Eh_0^4)^{-1}$, $\overline{w}=w/h_0$, $\overline{\varphi}=\varphi(Eh_0^3)^{-1}$, $\overline{x}_i=x_i/h_0$, $\overline{y}_i=y_i(Eh_0^3)^{-1}$, w_0 - initial imperfection (bars over non-dimensional quantities are further omitted).

In order to solve equations (8.13), where deflection w and the Airy's function φ are independently variated sought functions, we can not apply directly the Ritz procedure. In order to find the approximate values of w^0 and φ^0, we take the coordinate series $w_i(\alpha,\beta)$ and $\varphi_i(\alpha,\beta)$ $(i=1,2,3...)$. The approximate solution has the following form

$$w=\sum_{i=1}^{n}x_i(t)w_i(\alpha,\beta),\quad \varphi=\sum_{i=1}^{n}y_i(t)\varphi_i(\alpha,\beta). \tag{8.14}$$

The coefficients $x_i(t)$ and $y_i(t)$ are the being sought functions of time. After first variation procedure the following system of ODEs is obtained

$$\mathbf{A}(\ddot{\mathbf{X}}+\varepsilon\dot{\mathbf{X}})+\mathbf{BX}+\mathbf{CY}+\mathbf{DXY}=\mathbf{Q}q_0,\quad \mathbf{CX}+\mathbf{EY}+\frac{1}{2}\mathbf{DXX}=0, \tag{8.15}$$

where: $\mathbf{A}=\sum_{i=1}^{n}\sum_{j=1}^{n}A_{ij}$, $\mathbf{B}=\sum_{i=1}^{n}\sum_{j=1}^{n}B_{ij}$, $\mathbf{C}=\sum_{i=1}^{n}\sum_{j=1}^{n}C_{ij}$, $\mathbf{D}=\sum_{i=1}^{n}\sum_{j=1}^{n}D_{ij}$,
$\mathbf{E}=\sum_{i=1}^{n}\sum_{j=1}^{n}E_{ij}$, $\mathbf{X}=\sum_{i=1}^{n}x_i$, $\mathbf{Y}=\sum_{j=1}^{n}y_j$, $\mathbf{Q}=\sum_{i=1}^{n}Q_i$.

In what follows we study axially symmetric problem of closed (in their tops) shallow rotational shells and circled plates subjected to a surface distributed normal load. In polar coordinates and taking into account the axial symmetry we have $w=w(\rho)$, $\varphi=\varphi(\rho)$, $\alpha=r$, $\beta=\theta$, $ds=2\pi r dr$, and the shell thickness $\overline{h}=h(\rho)/h_0$, $h(\rho)=h_0(1+c\rho)$, and the used operators have the following form

$$\Delta=\frac{\partial^2}{\partial\rho}+\frac{1}{\rho}\frac{\partial}{\partial\rho},\quad L(w,\varphi)=\frac{\partial^2 w}{\partial\rho^2}\frac{1}{\rho}\frac{\partial\varphi}{\partial\rho}+\frac{1}{\rho}\frac{\partial w}{\partial\rho}\frac{\partial^2\varphi}{\partial\rho^2}.$$

Then deflection w and the stress function φ have the following form

$$w=\sum_{i=1}^{n}x_i(t)w_i(\rho),\quad \varphi=\sum_{i=1}^{n}y_i(t)\varphi_i(\rho), \tag{8.16}$$

and the coefficients of system (8.15) are as fallows

$$A_{ik}=\int_0^1(1+c\rho)w_i w_k\rho d\rho,$$
$$B_{ik}=\frac{1}{12(1-\nu^2)}\int_0^1(1+c\rho)^3\left[\Delta w_i\Delta w_k-(1-\nu)L_2(w_i,w_k)\right]\rho d\rho,$$
$$C_{ip}=-\int_0^1\left[\Delta_k\varphi_p+L_2(w_0,\varphi_p)\right]w_i\rho d\rho,\qquad Q_i=\int_0^1 w_i\rho d\rho, \tag{8.17}$$
$$D_{ikp}=-\int_0^1 w_i L_2(w_k,w_p)\rho d\rho,$$
$$E_{jp}=-\int_0^1\frac{1}{1+c\rho}\left[\Delta\varphi_j\Delta\varphi_p-(1+\nu)L_2(\varphi_j,\varphi_p)\right]\rho d\rho.$$

Solving (8.15) regarding y_i yields

$$\mathbf{Y}=\left[\mathbf{E}^{-1}\mathbf{C}+\frac{1}{2}\left(\mathbf{E}^{-1}\mathbf{DX}\right)\right]\mathbf{X}. \tag{8.18}$$

Multiplying by $\mathbf{A}^{-1}$ first equation of (8.15) and denoting by $\mathbf{X}=\mathbf{R}$, we obtain the following nonlinear Cauchy problem

$$\dot{\mathbf{R}}=-\bar{\varepsilon}\mathbf{R}+\left[\mathbf{A}^{-1}\mathbf{C}+\left(\mathbf{A}^{-1}\mathbf{DX}\right)\right]\cdot\mathbf{Y}-\mathbf{A}^{-1}\mathbf{BX}+q_0(\bar{t})\mathbf{A}^{-1}\mathbf{Q},\quad \dot{\mathbf{X}}=\mathbf{R}. \tag{8.19}$$

Observe that the so far applied transformation is allowed, because the matrices $\mathbf{A}^{-1}$ and $\mathbf{E}^{-1}$ do exist if the coordinate functions are linearly independent. Equations (8.19) with the initial conditions

$$x_i = 0, \quad \dot{x}_i = 0 \qquad \text{for} \qquad t = 0$$

have been solved by the 4-th order Runge-Kutta method.

The system of the used approximating functions for four applied boundary conditions is reported in Tab. 8.1.

Tab. 8.1. Approximating functions

$\varphi_j(\rho)$	$w_i(\rho)$	
	$(1-\rho^2)^{i+1}$	$(1-\rho^2)^{i}$
ρ^{2j}	Fixed clamping	Fixed free support
$(1-\rho^2)^{j+1}$	Movable clamping	Movable free support

We study vibrations of a conical shallow shell as a plate with initial deformation $w_0 = -k(1-\overline{\rho})$, $k = H/h_0$ and the system equations for the mentioned four boundary conditions follow:

1. Non-movable clamping

$$A_{ik}^{(1)} = \frac{1}{6+2i+2k} + c\frac{(4+2i+2k)!!}{(7+2i+2k)!!},$$

$$B_{ik}^{(1)} = \frac{4(i+1)(k+1)}{3(1-\nu^2)}\left\{\frac{1}{i+k+1}\left\{\frac{ik}{(i+k)(i+k+1)} + \right.\right.$$

$$\left.\left. + \frac{3c^2}{2(i+k+2)}\left[\frac{6ik}{(i+k)(i+k-1)} - \frac{1+\nu}{2}\right]\right\} + \frac{3c(2i+2k-4)!!}{(2i+2k+3)!!}\left[15ik - (1+\nu)(i+k)(i+k-1)\right]\right\},$$

$$C_{ip}^{(1)} = -2(p+1)\cdot\frac{H}{h_0}\left(-\int_0^1 (1-\rho^2)^{i+p+1}\,d\rho + 2p\int_0^1 \rho^2\left(1-\rho^2\right)^{i+p}\,d\rho\right), \tag{8.20}$$

$$E_{jp}^{(1)} = 4ip\left[(j+p-1)(1+\nu) - 2jp\right]\left(\frac{1}{j+p-1} - \frac{c}{j+p-1/2} + \frac{c^2}{j+p}\right),$$

$$D_{ikp}^{(1)} = 4(i+1)(k+1)\,p\frac{p!}{(i+k+1)\ldots(i+k+p+1)}, \qquad Q_i = \frac{1}{2(i+2)}.$$

2. Movable clamping

$$A_{ik}^{(2)} = A_{ik}^{(1)}, \qquad B_{ik}^{(2)} = B_{ik}^{(1)},$$

$$C_{ip}^{(2)} = 2\frac{H}{h_0}\cdot p(2p-1)\cdot\int_0^1 \rho^{2p-2}\cdot(1-\rho^2)^{i+1}d\rho,, \qquad Q_i^{(2)} = Q_i^{(1)},$$

$$E_{jp}^{(2)} = -16(j+1)(p+1)\left\{\frac{pj}{(j+p+1)(j+p)(j+p-1)} + \frac{c^2}{2(j+p+1)(j+p+2)}\times\right.$$

$$\left.\times\left[\frac{6jp}{(j+p)(j+p-1)} - \frac{1-\nu}{2}\right] - c\frac{(2j+2p-4)!!}{(2j+2p+3)!!}\left[15jp - (1-\nu)(j+p)(j+p-1)\right]\right\},$$

$$D_{ikp}^{(2)} = -\frac{4(i+1)(k+1)(p+1)}{(i+k+p+1)(i+k+p+2)}. \tag{8.21}$$

3. Non-movable free support

$$A_{ik}^{(3)} = A_{i-1,k-1}^{(1)},$$

$$B_{ik}^{(3)} = \begin{cases} \dfrac{2+c(4+3c)}{6(1-\nu)}, & k = i = 1, \\ -\dfrac{c(4+5c)}{15(1-\nu)}, & i = 1, \quad k = 2; \quad i = 2, \quad k = 1, \\ B_{i-1,k-1}^{(1)}, & \end{cases} \tag{8.22}$$

$$C_{ip}^{(3)} = C_{i-1,p}^{(1)}, \quad D_{ikp}^{(3)} = D_{i-1,k-1,p}^{(1)}, \quad Q_i^{(3)} = Q_{i-1}^{(1)}, \quad E_{jp}^{(3)} = E_{jp}^{(1)}.$$

4. Movable free support

$$A_{ik}^{(4)} = A_{i-1,k-1}^{(1)}, \qquad B_{ik}^{(4)} = B_{ik}^{(3)}, \qquad C_{ip}^{(4)} = C_{i-1,p}^{(2)},$$
$$D_{ikp}^{(4)} = D_{i-1,k-1,p}^{(2)}, \qquad Q_i^{(4)} = Q_{i-1}^{(1)}, \qquad E_{jp}^{(4)} = E_{jp}^{(2)}. \tag{8.23}$$

During investigation of the spherical shell we treat it as a plate with initial deflection $w_0 = -k(1-\rho^2)$. For all four types of boundary conditions shown in Tab. 8.1 the coefficients of system (8.19) differ from the case of conical shell only regarding the coefficients C_{ip}, which follow:

1. Non-movable clamping: $\qquad C_{ip}^{(1)} = -4\dfrac{H}{h_0}p\dfrac{(1+i)!\,p!}{(i+p+1)!}$;

2. Movable clamping: $C_{ip}^{(2)} = 4\frac{H}{h_0}(i+1)(p+1)\frac{(i+p)!}{(i+p+2)!}$;

3. Non-movable free support: $C_{ip}^{(3)} = C_{i-1,p}^{(1)}$;

4. Movable free support: $C_{ip}^{(4)} = C_{i-1,p}^{(2)}$.

The defined so far Cauchy problem will be solved using the Runge-Kutta method of fourth order and the following harmonic excitation $q=q_0\sin\omega_p t$ is applied.

8.4. Shells of infinite length

In this Section we study elastic isotropic infinite shells, having the material obeying the Hooke's law by taking into account their geometrical nonlinearity, i.e. the relation between deformations and displacements is of the following form:

$$\varepsilon_x = \frac{\partial u}{\partial x} - k_x w + \frac{1}{2}\left(\frac{\partial w}{\partial x}\right)^2. \tag{8.24}$$

Full deformations of an arbitrary shell point regarding shell thickness ε_x^z is composed of deformations of the middle surface ε_x and bending deformations ($\varepsilon_x^z = \varepsilon_x + \varepsilon_{x,u}$), which according the Kirchhoff-Love hypothesis read

$$\varepsilon_{x,u} = -z\frac{\partial^2 w}{\partial x^2}. \tag{8.25}$$

Consider the shell motion in time interval of t_0 and t_1. In what follows we compare for this time interval various trajectories of the shell points between initial and end points position. Real trajectories are distinguished from other ones by the following relation to be satisfied:

$$\int_{t_0}^{t_1}(\delta K - \delta\Pi + \delta' W)dt = 0. \tag{8.26}$$

Here by K we mean kinetic system energy, by Π we denote its potential energy, whereas $\delta' W$ is the sum of elementary works of external forces.

In this case and assuming that all forces acting on the system have a potential, the relation (8.26) yields:

$$\delta S = \delta\int_{t_0}^{t_1}(K-\Pi)dt = 0, \tag{8.27}$$

where $S = \int_{t_0}^{t_1}(K-\Pi)\partial t$ is the Hamilton action. After the standard transformations, the following non-dimensional equations regarding displacements are obtained

$$\begin{gathered}\frac{\partial^2 u}{\partial x^2} - k_x\frac{\partial w}{\partial x} + \frac{\partial w}{\partial x}\frac{\partial^2 w}{\partial x^2} + p_x - \frac{\partial^2 u}{\partial t^2} = 0,\\ -\frac{1}{12}\frac{\partial^4 w}{\partial x^4} + \frac{\partial w}{\partial x}\left(\frac{\partial^2 u}{\partial x^2} - k_x\frac{\partial w}{\partial x} + \frac{\partial w}{\partial x}\frac{\partial^2 w}{\partial x^2}\right) +\\ +\left(k_x + \frac{\partial^2 w}{\partial x^2}\right)\left(\frac{\partial u}{\partial x} - k_x\frac{\partial w}{\partial x} + \frac{1}{2}\left(\frac{\partial w}{\partial x}\right)^2\right) + q - \frac{1}{12}\frac{\partial^2 w}{\partial t^2} - \varepsilon\frac{\partial w}{\partial t} = 0.\end{gathered} \tag{8.28}$$

Transformation to non-dimensional form is realized using the following relations:

$$\begin{gathered}\bar{k}_x = \frac{a}{R_x}\frac{1}{\lambda},\quad p_x = \frac{E}{1-\nu^2}\lambda^3\bar{p}_x,\quad q = \frac{E}{1-\nu^2}\lambda^4\bar{q},\quad \lambda = \frac{h}{a},\\ t = a\sqrt{\frac{(1-\nu^2)\gamma}{Eg}}\bar{t},\quad u = \bar{u}\lambda^2,\quad x = a\bar{x},\end{gathered} \tag{8.29}$$

where bars correspond to non-dimensional quantities, and in equations (8.28) they have been already omitted. In relations (8.29) E denotes the elasticity modulus, ν is Poisson's coefficient, γ denotes volume unit material weight, g is the Earth acceleration, q is the transversal load being the function of x and t, h and a – are thickness and linear shell dimension respectively, w and u are deflection and displacement of the shell middle surface, and k_x=1/R_x is the shell curvature.

The following boundary and initial conditions are supplemented to equations (8.28):

Boundary conditions:

1. Free non-movable support:

$$u = w = \frac{\partial^2 w}{\partial x^2} = 0, \text{ for } x = 0;\ 1. \tag{8.30}$$

2. Stiff support:

$$u = w = \frac{\partial w}{\partial x} = 0, \text{ for } x = 0;\ 1. \tag{8.31}$$

3. Hybrid support:

for $x = 0$ $\quad u = w = \dfrac{\partial^2 w}{\partial x^2} = 0$ - free-non-movable support;

for $x = 1$ $\quad u = w = \dfrac{\partial w}{\partial x} = 0$ - stiff clamping. (8.32)

The initial conditions for t = 0 read:

$$u = f_1(x), \quad \dot{u} = f_2(x), \quad w = f_3(x), \quad \dot{w} = f_4(x). \tag{8.33}$$

We approximate the partial derivative regarding x in equations (8.28) by difference relations with error $O(h_1^4)$ using for this purpose the Taylor series in a neighborhood of the point x_i with steps h_1, where h_1 is the partition step and $x \in [0,1]$:

$$G_{h_1} = \{0 \le x_i \le 1, x_i = ih_1, i = \overline{0,N}, h_1 = \frac{1}{N}\}.$$

In this case the partial differential equations (8.29) are transformed to ordinary differential second order equations in time for the i–th point of the interval [0, 1].

The boundary and initial conditions are as follows:

(i) Boundary conditions:

1. Free non-movable support:

$$u_i = w_i = \Lambda_{x^2}(w_i) = 0, \quad i = 0; N. \tag{8.34}$$

2. Stiff clamping of the shall boundaries:

$$u_i = w_i = \Lambda_x(w_i) = 0, \quad i = 0; N. \tag{8.35}$$

(ii) Initial conditions:

$$u_i = f_1(ih_1), \quad \dot{u}_i = f_2(ih_1), \quad w_i = f_3(ih_1), \quad \dot{w}_i = f_4(ih_1). \tag{8.36}$$

The obtained system of second order ODEs we transform to first order ones, and then we solve it by the 4-th order Runge-Kutta method.

8.5. Transitions from regularity to chaos

A transition of a continual mechanical system from periodic to chaotic vibrations via the Feigenbaum scenario has been detected during investigations of vibrations of axially symmetric, cylindrical and conical shells.

In order to investigate shells periodically driven a special numerical algorithm has been proposed for constructing of the so called vibration-type charts in the control parameters plane $\{q_0, \omega_p\}$. The vibration type identification of the cylindrical shell during construction of the chart $\{q_0, \omega\}$ for each signal $w(t)$ has been carried out using analysis of the frequency power spectrum $S(\omega)$ and the Lyapunov exponents. Those charts allow to investigate the whole dynamics in plane $\{q_0, \omega_p\}$. The used approach can clearly separate the Feigenbaum scenarios, the modified Ruelle-Takens-Newhouse scenarios, and the subspaces of the Ruelle-Takens-Newhouse-Feigenbaum scenario.

Initially we study a problem of convergence of a solution during increase of a number of partition of the control parameter plane $\{q_0, \omega_p\}$. In order to construct such charts we put on the plane $\{q_0, \omega_p\}$ a grid, nodes of which have been used for the vibration type identification, i.e. one needs to solve the corresponding dynamical problem, construct and analyze the frequency spectra and the Lyapunov exponents for each of the grid points (nodes). The computations have shown that for $N \times N \ge 350 \times 350$ the choice of nodes number is optimal one for the periodic and chaotic subspaces of the vibration charts versus the control parameters $\{q_0, \omega_p\}$. The charts allow to study all dynamic properties of the construction and choose the most suitable excitation parameters. Investigating a chart, one may know which frequencies of excitations correspond to periodic vibrations, i.e. vibrations being not dangerous for the construction. On the other hand the Andronov-Hopf bifurcations and 2D quasi-periodic orbits correspond to transitional zones. In addition, one may separate zones of chaotic vibrations, most important for application. Besides the

charts of the vibration-type character versus control parameters $\{q_0, \omega_p\}$, the charts of a "stiff" stability loss regarding the same parameters have been constructed.

8.6. Concluding remarks

In Fig. 8.1 two overlapped charts for the case of conical movably clamped shell with k=5 are reported. A solution has been obtained by the Ritz method in higher approximations (white points of the chart correspond to the system stability loss).

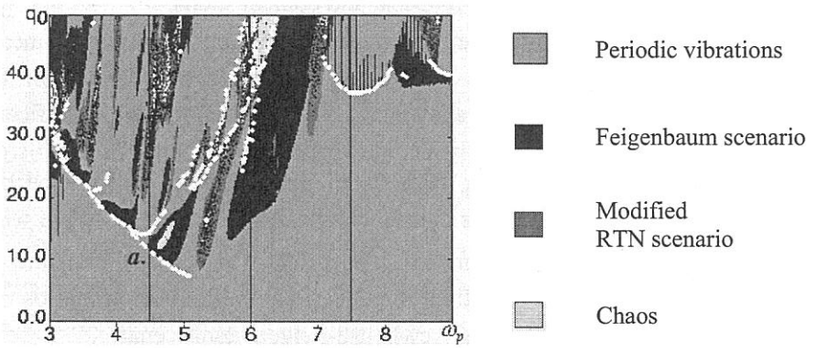

Fig. 8.1. Charts of the vibration-type character versus control parameters $\{q_0, \omega_p\}$ (stiff stability loss)

One may conclude from Fig. 8.1, that stiff stability loss occurs during the change of vibration character. However, there exist points within a zone of periodic vibrations, where a stiff stability loss is observed. More detailed numerical analysis has shown that in those points instead of the first order discontinuities (Fig. 8.2a), we have a deflection point (Fig. 8.2b) of the function $w_{\max}(q)$.

We investigate the problem on the modes number in the Ritz procedure using example of vibrations of conical shallow geometrically nonlinear shells of constant thickness, movably clamped on their contours. The load is uniformly distributed on the shell surface in the following harmonic way $q=q_0\sin\omega_p t$.

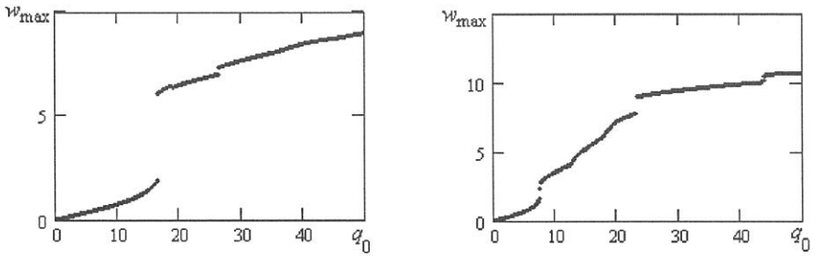

a) ω_p=4 b) ω_p=5

Fig. 8.2. Dependence $w_{\max}(q)$

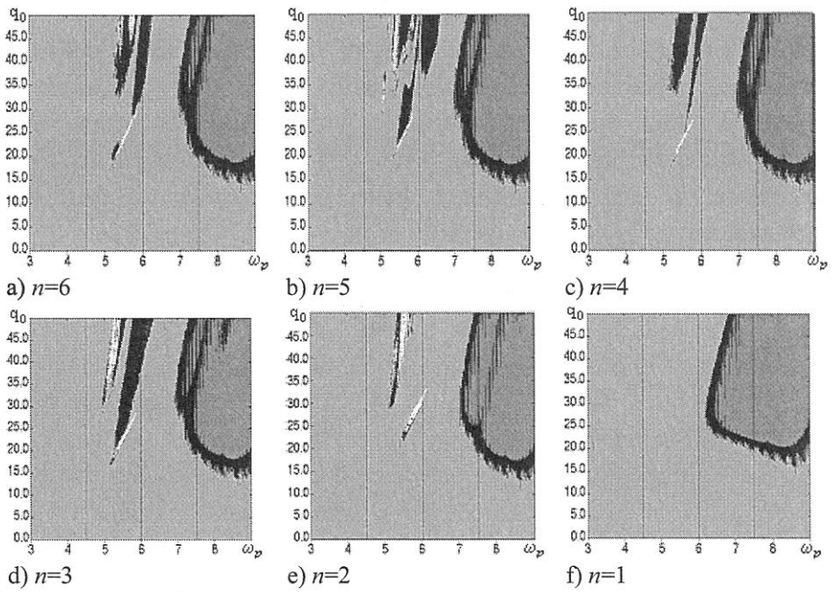

Fig. 8.3. Charts of the vibration-type characters in the control parameters plane $\{q_0, \omega_p\}$ (movably clamped conical shell for k=3)

Let us construct charts of the shell with height arrow k=3 and k=5 (Fig. 8.3) depending on the magnitudes of the control parameters $\{q_0, \omega_p\}$ for various numbers of the series terms n=1,...,6 in (8.14). Further increase of n in (8.14) does not caused a qualitative change of the charts $\{q_0, \omega_p\}$. Notation of the vibration type zones are given in the figures, and zones of the modified

Ruelle-Takens-Newhouse scenario are not reported here. The choice of a magnitude of the loading parameter q_0 is limited by a shell deflection in frame of the given applied theory. Parameter ω_p is changed from $\omega_0/2$ to $3\omega_0/2$, where ω_0 is free vibration frequency. Chart n=1 presented in Fig. 8.3 differs from other ones mainly by a lack of chaotic zones and exhibits only zones of bifurcations and periodic vibrations with frequencies ω_p and $0.5\omega_p$. Increase of n yields occurrence of new bifurcations and chaotic zones, parts of which do not undergo any changes beginning from n=3 (for instance, zones of bifurcation and periodic vibrations with fundamental frequency $0.5\omega_p$ in higher frequency zones). Chart for n=1 strongly differs from other ones, and increasing n outlines that various zones are similar, i.e. a convergent series of vibration sequence is observed. Sub-harmonic vibrations zone with $0.5\omega_p$ is the same for all $n\geq2$, however for n=2 it is shifted into the right. Chaotic zones with increase of n become smaller, but the separated parts beginning from n=4 do not change. In general, convergence on high frequencies is better in comparison to that of low frequencies and being close to eigenfrequency.